PROCEEDINGS OF SCIENCE

Nucleon electromagnetic form factors at large momentum from Lattice QCD

S. Syritsyn,[a,*] **M. Engelhardt,**[b] **S. Krieg,**[c,d,e] **J. Negele**[f] **and A. Pochinsky**[f]

[a] *Department of Physics & Astronomy, Stony Brook University, 1 Nicolls Rd, Stony Brook, NY 11733, USA*
[b] *Department of Physics, New Mexico State University, Las Cruces, NM 88003, USA*
[c] *Jülich Supercomputing Centre, Forschungszentrum Jülich, 52425 Jülich, Germany*
[d] *Helmholtz-Institut für Strahlen- und Kernphysik, Universität Bonn, 53115 Bonn, Germany*
[e] *Center for Advanced Simulation and Analytics (CASA), Forschungszentrum Jülich, 52425 Jülich, Germany*
[f] *Center for Theoretical Physics, Massachusetts Institute of Technology, 77 Massachusetts Ave., Cambridge, MA 02139, USA*

E-mail: sergey.syritsyn@stonybrook.edu

Proton and neutron electric and magnetic form factors are the primary characteristics of their spatial structure and have been studied extensively over the past half-century. At large values of the momentum transfer Q^2 they should reveal transition from nonperturbative to perturbative QCD dynamics as well as effects of quark orbital angular momenta and diquark correlations. Currently, these form factors are being measured at JLab at momentum transfer up to $Q^2 = 18$ GeV^2 for the proton and up to 14 GeV^2 for the neutron. We report preliminary results of our lattice calculations of these form factors, including G_E and G_M nucleon form factors with momenta up to $Q^2 = 8$ GeV^2, pion masses down to the almost-physical m_π=170 MeV, several lattice spacings down to $a = 0.073$ fm, and high $O(10^5)$ statistics. Specifically, we study individual form factors, the G_E/G_M ratios, and flavor dependence of contributions to the form factors. We observe qualitative agreement of our ab initio theory calculations with experiment. Comparison of our calculations and upcoming JLab experimental results will be an important test of nonperturbative QCD methods in the almost-perturbative regime.

The 41st International Symposium on Lattice Field Theory (LATTICE2024)
28 July - 3 August 2024
Liverpool, UK

*Speaker

PoS(LATTICE2024)340

1. Introduction

Nucleon electromagnetic form factors $G_{Ep,n}$, $G_{Mp,n}(Q^2)$ at high momentum transfer $Q^2 \approx 5\ldots10\,\mathrm{GeV}^2$ describe short-scale spatial distributions of electric charge and magnetization and are crucial to our understanding of nucleon structure and improving nucleon models. In general, they are defined as nucleon matrix elements of the vector current,

$$\langle N(p',S')|\bar{q}\gamma^\mu q|N(p,S)\rangle = \bar{u}_{p',S'}\left[F_1(Q^2)\gamma_\mu + F_2(Q^2)\frac{i\sigma^{\mu\nu}(p'-p)_\nu}{2m_N}\right]u_{p,S} \tag{1}$$
$$\text{and } G_E(Q^2) = F_1(Q^2) - \frac{Q^2}{4M^2}F_2(Q^2)\,,\quad G_M(Q^2) = F_1(Q^2) + F_2(Q^2)\,,$$

for spacelike $Q^2 = -(p'-p)^2 \geq 0$. Various models such as vector meson dominance, chiral solitons, pion cloud, and relativistic constituent quarks have been tried to predict form factor behavior at large Q^2. While these models generally describe available form factor data, their predictions differ outside of experimentally explored range of momenta [1]. It has also been shown using Dyson-Schwinger and Faddeev equations that incorporating diquark correlations is important for understanding nucleon electromagnetic structure at high momentum transfer [2]. For example, quark correlations in the Faddeev's amplitude of the proton determine if there is indeed a peculiar zero-crossing in the electric Sachs form factor G_{Ep} around $Q^2 \approx 8.5\mathrm{GeV}^2$, and thus can be inferred from experimental or nonperturbative lattice form factor data. The experimental program to determine nucleon form factors up to $Q^2 \approx 18\,\mathrm{GeV}^2$ is well underway [3–7], and the first results have been published for the proton magnetic form factor $G_{Mp}(Q^2)$ for Q^2 up to $\approx 16\,\mathrm{GeV}^2$ [8]. Our ongoing lattice calculations of the nucleon form factors are intended to complement these experimental efforts, and have to be performed with rigorous control of all systematic uncertainties.

Mainstream studies of nucleon form factors on a lattice are usually limited to the region $Q^2 \lesssim 1\ldots2\,\mathrm{GeV}^2$. One notable exception is the calculation of the G_{Ep}/G_{Mp} ratio using the Feynman-Hellman method [9]. Precise calculation of nucleon structure involving large momenta $|\vec{p}| \gtrsim m_N$ are challenging for several reasons. With growing energy of the in- and out-states, Monte Carlo fluctuations of the corresponding correlators increase rapidly [10], and the signal-to-noise ratio decreases $\propto \exp\left[-(E_N(\vec{p}) - \frac{3}{2}m_\pi)\tau\right]$ with Euclidean time τ. At the same time, systematic uncertainties from nucleon excited states have weaker suppression as the energy gaps $\Delta E(\vec{p}) = E_{N,\mathrm{exc}}(\vec{p}) - E_N(\vec{p})$ shrink due to the relativistic dispersion relation. Both these challenges can be minimized by choosing the Breit frame on a lattice, so that the initial and final momenta of the nucleon are equal to $|\vec{p}^{(\prime)}| = \frac{1}{2}\sqrt{Q^2}$. Still, the minimal nucleon momentum to achieve $Q^2_1 \approx 10\,\mathrm{GeV}^2$ is $p_1 \gtrsim 1.6\,\mathrm{GeV}$ and results in reducing the typical excitation energy gap $\Delta E_N(0) \approx 0.5\,\mathrm{GeV}$ to $E_N(p_1) \approx 0.3\,\mathrm{GeV}$, which is challenging even if pion-nucleon states are not considered. These problems are compounded in computing quark-disconnected nucleon-current correlators, which could yield substantial contributions to the nucleon form factors at $Q^2 \gtrsim 1\,\mathrm{GeV}^2$. Therefore, very large Monte Carlo statistics combined with rigorous analysis of excited states are crucial for obtaining credible results.

Over a few years, we have accumulated significant Monte Carlo statistics on nucleon-current correlators with momentum transfer values $Q^2 \lesssim 8\,\mathrm{GeV}^2$ (and larger in some cases) at a range of lattice spacings, as well as quark masses that approach the physical point. Some of our initial

results have been previously reported in Refs. [11–13]. More recently, we have also accumulated substantial statistics on the disconnected quark loops. In this paper, we report and compare these disconnected contributions to the connected contributions on two ensembles, one of which is very close to the physical pion mass.

2. Lattice setup

We have performed large-statistics calculations on four ensembles of lattice gauge fields. We use gauge configurations generated with $N_f = 2 + 1$ dynamical quarks with isotropic clover-improved Wilson fermion action by the JLab/W&M/LANL/MIT groups. Our ensemble parameters and accumulated statistics are summarized in Tab. 1. Because discretization effects are potentially significant at large momentum, we use a range of lattice spacings $a \approx 0.07 \ldots 0.09\,\text{fm}$, with some earlier calculations performed at the coarse $a \approx 0.127\,\text{fm}$. While the quark masses should have only limited effect at the scale of $Q^2 \gtrsim 1\,\text{GeV}^2$, they may affect energies of excited states contributing to systematic effects, therefore we study two values of the pion mass, $m_\pi \approx 280$ and 170 MeV. Calculations at the lighter pion mass require substantially more statistics; we illustrate the comparison of accumulated data sample counts in Fig. 1.

Table 1: Summary of ensembles, form factor kinematic ranges, and statistics. The columns 5,6,7 show the total number of gauge configurations analyzed, the number of connected correlator MC samples, and the number of gauge configurations on which disconnected contributions have been calculated.

ens	lat	a [fm]	m_π [MeV]	Nconf	$N_{\text{stat}}^{\text{conn}}$	$N_{\text{conf}}^{\text{disc}}$	t_{sep}/a	t_{sep} [fm]	Q^2_{max} [GeV^2]
C13	$32^3 \times 96$	0.127	285	210	20,160	–	6 . . . 10	1.27	8.3
D5	$32^3 \times 64$	0.094	278	1346	86,144	1346	6 . . . 12	1.13	10.9
D6	$48^3 \times 96$	0.091	166	2040	261,120	1152	6 . . . 12	1.09	8.0
E5	$48^3 \times 128$	0.073	272	2080	266,240	–	7 . . . 14	1.02	8.0

In order to calculate the nucleon form factors, we evaluate nucleon-current correlators using the standard sequential propagator method,

$$C_{N V_q^\mu \bar{N}}(\vec{p}', \vec{q}; t_{\text{sep}}, t_{\text{ins}}) = \sum_{\vec{y},\vec{z}} e^{-i\vec{p}'\vec{y}+i\vec{q}\vec{z}} \left\langle N_{(\vec{k})}(\vec{y}, t_{\text{sep}}) \, [\bar{q}\gamma^\mu q]_{\vec{z},t_{\text{ins}}} \, N_{(-\vec{k})}(0) \right\rangle , \tag{2}$$

where $N_{\pm\vec{k}} = \epsilon^{abc} [\tilde{u}^{aT}_{(\pm\vec{k})} C\gamma_5 \tilde{d}^b_{(\pm\vec{k})}] \tilde{u}^c_{(\pm\vec{k})}$ is the nucleon interpolating field on a lattice constructed with "momentum-smeared" quark fields $\tilde{q}_{(\pm\vec{k})}$, $\vec{k} \uparrow\uparrow \vec{p}'$, to improve their overlap with the ground states of the boosted in- and out-nucleon [14]. Wick contractions of lattice quark fields generate two types of diagrams: quark-connected and quark-disconnected. At momenta $Q^2 \lesssim 1\,\text{GeV}^2$, the form factors are dominated by the connected contributions discussed in Sec 3. The quark-disconnected contributions are calculated as correlators between nucleon 2-point Wick contractions and the quarks loops and are discussed in Sec. 4. Although the contributions of the latter were found small ($\lesssim 1\%$) at $Q^2 \lesssim 1\,\text{GeV}^2$ [15], they have to be explored at higher momenta as they can contribute to systematic uncertainty.

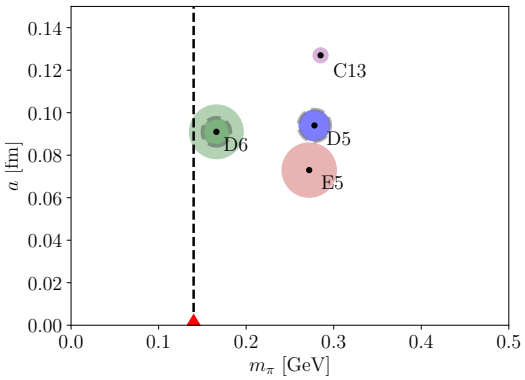

Figure 1: Summary of statistics accumulated so far in out study of the form factors. The circle area is proportional the number of lattice correlator samples: the solid- and dashed-border circles refer to the sample counts for the connected and disconnected contributions, respectively.

Nucleon matrix elements and form factors are extracted from nucleon-current three-point correlation functions using standard methods of lattice QCD (see, e.g. Ref. [16]). We use the two-state model for both two- and three-point correlators,

$$\langle N(\vec{p},t)\bar{N}(0)\rangle \sim C_0^2 e^{-E_{N0}t} + C_1^2 e^{-E_{N1}t}\,, \tag{3}$$

$$\begin{aligned}\langle N(\vec{p}',t)J(\vec{q},\tau)\bar{N}(0) \sim{}& \mathcal{A}_{0'0}C_{0'}C_0 e^{-E'_{N0}(t-\tau)-E_{N0}\tau} + \mathcal{A}_{1'0}C_{1'}C_0 e^{-E'_{N1}(t-\tau)-E_{N0}\tau} \\ &+ \mathcal{A}_{0'1}C_{0'}C_1 e^{-E'_{N0}(t-\tau)-E_{N1}\tau} + \mathcal{A}_{1'1}C_{1'}C_1 e^{-E'_{N1}(t-\tau)-E_{N1}\tau}\end{aligned} \tag{4}$$

to find ground-state nucleon energies $E^{(\prime)}_{N0}$, matrix elements of nucleon operators $C_{0^{(\prime)}} = \langle \mathrm{vac}|N|N(\vec{p}^{(\prime)})\rangle$, and matrix elements of the vector current $\mathcal{A}_{0'0} = \langle N(\vec{p}')|J|N(\vec{p})\rangle$. The two-point correlators and the ground-state energies are shown in Fig. 2. The dispersion relation $E^2(p^2)$, also shown in Fig. 2, is in good agreement with the continuum $E^2(p) = E^2(0) + p^2$, indicating that discretization effects on the spectrum of moving nucleons are insignificant.

3. Connected contributions

The ground-state matrix elements $\mathcal{A}^q_{0'0}$ from fits (4) are decomposed into form factors $F^q_{1,2}$ (1) separately for flavors u and d. Light-flavor connected combinations corresponding to the proton and the neutron form factors are shown in Fig. 3, and compared to phenomenological fits [17]. Although our lattice results have qualitatively similar Q^2 behavior to the phenomenological fits, they overshoot the latter by a factor of $(2\ldots2.5)$.

This substantial difference may be due to any combination of excited state contributions, discretization effects, and omission of disconnected contributions. Of these three potential sources, the excited state effects will likely be the most difficult to control. Our calculations with two lattice spacings $a = 0.091$ and 0.073 fm offer some insight into the magnitude of discretization effects. In particular, the Dirac F_1 form factor appears less affected by them compared to the Pauli F_2 form factor. This difference can be attributed to how these form factors contribute to the vector current matrix elements: unlike the Dirac F_1, the Pauli F_2 form factor contributes proportionally

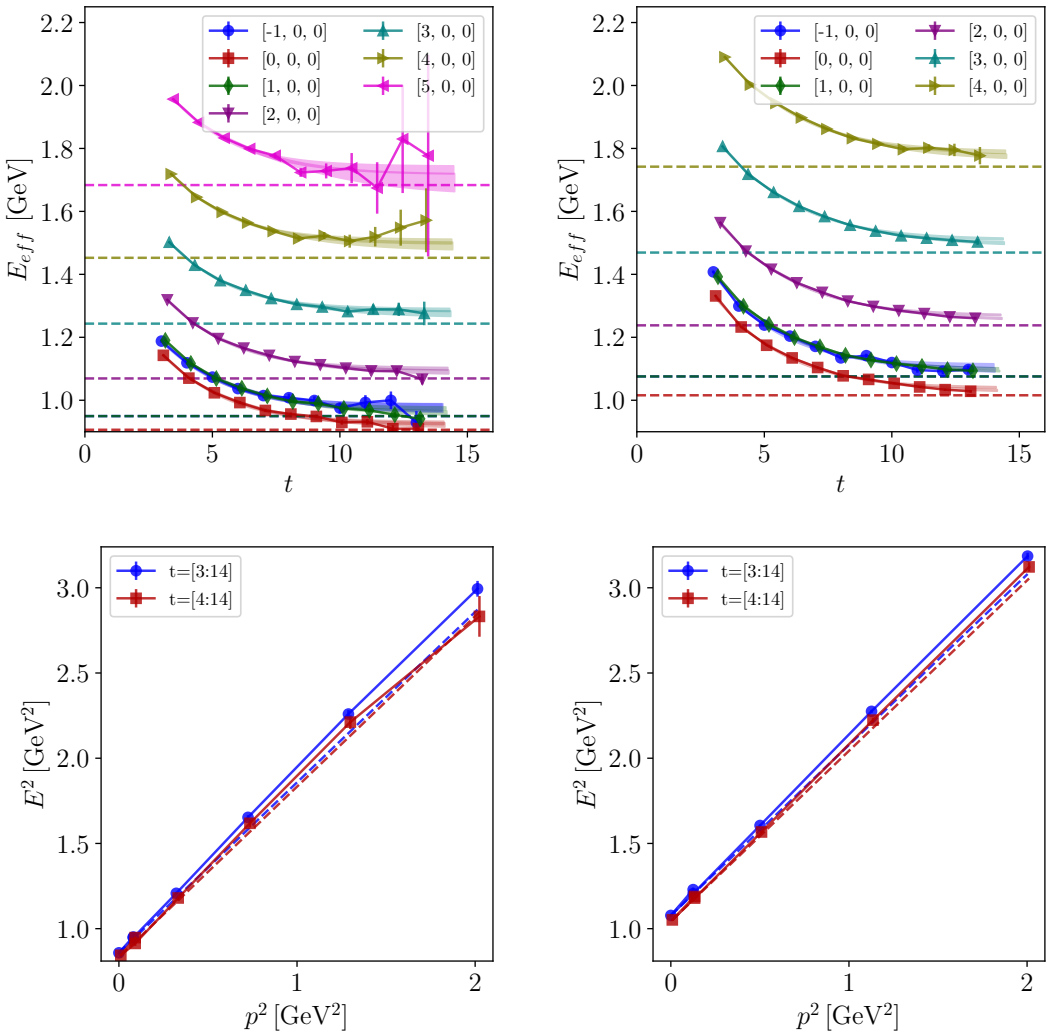

Figure 2: The effective energy (top) and the dispersion relation of the nucleon (bottom) determined on the D6 ($m_\pi \approx 170\,\text{MeV}$, $a \approx 0.091\,\text{fm}$)) (left) and the E5 ($m_\pi \approx 270\,\text{MeV}$, $a \approx 0.073\,\text{fm}$)) (right) ensembles. The dashed lines show the continuum dispersion relation with the mass determined from the lattice.

to the momentum transfer $\propto \sigma_{\mu\nu} q^\nu$. A detailed study of $O(a)$-improved current operators and calculations at additional values of lattice spacings planned in the future will be highly beneficial for exploring these effects.

4. Disconnected contributions

The main part of the present work is evaluating the magnitude of disconnected contributions to the high-momentum nucleon form factors for the first time. The nucleon-nucleon part of the Wick contractions in Eq. (2) is evaluated simultaneously with the connected 3-point correlators. The "quark loops"

$$\sum_{\vec{z}} e^{i\vec{q}\vec{z}} \langle \bar{q}_z \Gamma q_z \rangle_{\text{Wick}} = -\text{Tr}\left[\Gamma \not{D}^{-1}\right] \tag{5}$$

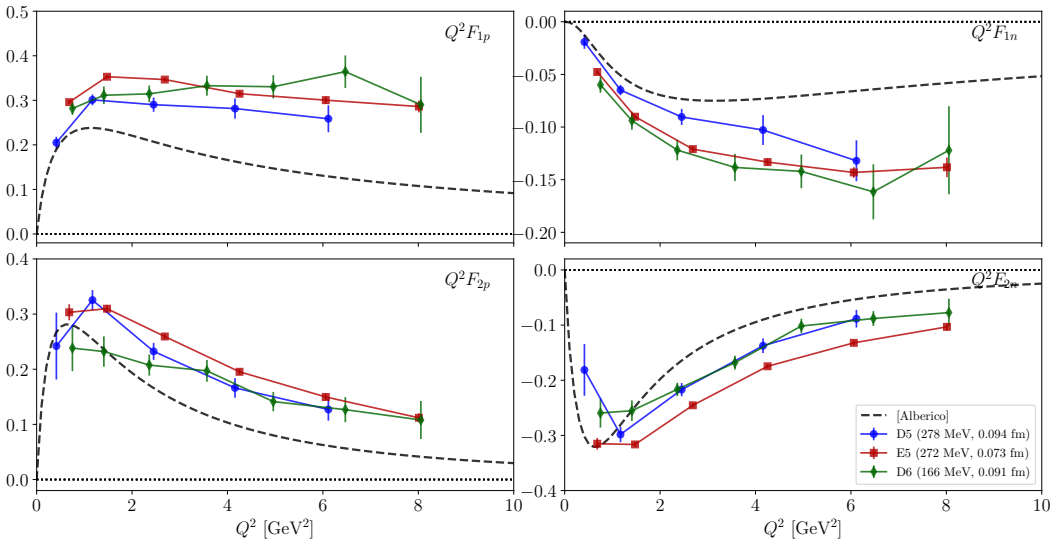

Figure 3: Comparison of the Dirac F_1 (top) and the Pauli F_2 (bottom) form factors of the proton (left) and the neutron(right) computed on three ensembles D5, D6, and E5 (connected contributions only). Ground-state matrix elements are extracted with 2-state fits to two- and three-point correlators using data with source-sink separations $t_{\rm sep} = 0.7 \ldots 1.1$ fm. The dashed lines show phenomenological fits [17].

have to be calculated separately by (partially) stochastic methods. To do that, we employ hierarchical probing combined with deflation of the $(\not{D}^\dagger \not{D})$ operator [18, 19]. On each configuration, we calculate $N_{vec} = 400$ low-lying eigenmodes that are used for (1) exact evaluation of their contributions to Eq. (5) and (2) deflation of hierarchical probing vectors [18] that results in a substantial reduction of the variance in the stochastic estimation of the high-mode part. We use $N_{hp} = 512$ spatial hierarchical probing vectors on each configuration that result in exact cancellation of variance contributions up to distance of $2a$ in each of the 4 directions.

We have calculated disconnected quark loops and their contributions to the form factors on the D5 and D6 ensembles, with full and $\approx 1/2$ statistics respectively. First we examine the magnitude of these disconnected contractions relative to the connected contributions. Since our current goal is to examine how much these disconnected contractions and their uncertainties will affect the final result, we resort to using simple plateau-center averages as approximate estimators of the ground-state matrix elements. In Figure 4, we show the ratio of the disconnected to u quark-connected contributions to the form factors F_1 and F_2 obtained on the D6 ensemble with a range of source-sink separations $t_{\rm sep}$. We show separately the cases of disconnected light (L), strange (S), and the $[L-S]$ flavor combinations. In all cases, the values are statistically compatible with zero. However, the statistical uncertainties grow dramatically with increasing source-sink separation $t_{\rm sep}$, showing that it will be extremely challenging to constrain these contributions especially if excited states play a significant role. It is nevertheless reassuring that the $[L-S]$ flavor combination that contributes to

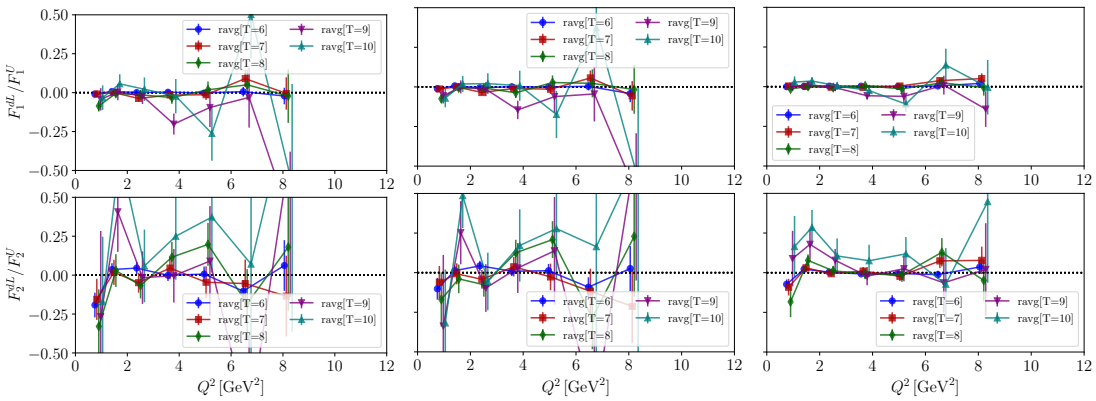

Figure 4: Comparison of connected and disconnected contributions to the Dirac F_1 and Pauli F_2 form factors of the proton on the D6 ($m_\pi \approx 170\,\mathrm{MeV}$) ensemble: (left) light flavors L, (middle) strange flavor S and (right) the combination $(L - S)$ occurring in the proton and the neutron. Note that statistical fluctuations cancel substantially in the latter.

the proton (P) and neutron (N) form factors,

$$\begin{aligned} P &= \frac{1}{3}[2U - D]_{\mathrm{conn}} + \frac{1}{3}[L - S]_{\mathrm{disc}}\,, \\ N &= \frac{1}{3}[2D - U]_{\mathrm{conn}} + \frac{1}{3}[L - S]_{\mathrm{disc}}\,, \end{aligned} \tag{6}$$

has the smallest statistical uncertainties due to partial noise cancellation. In particular, we expect that statistical uncertainty in F_1 due to disconnected contributions will be $\lesssim 20\%$ for Q^2 up to $8\,\mathrm{GeV}^2$, unlike in individual flavor form factors $F_{1,2}^{u,d,s}$, which will be more challenging to compute with high precision.

Finally, in Figure 5 we show our preliminary results for the proton and the neutron form factor ratios G_E/G_M with both connected and disconnected contributions included. As in our previous calculations, the ratios are much closer to the phenomenological fits despite the disagreement in the individual form factors. On the D6 ensemble, which is the closest one to the physical point, we observe qualitative agreement with phenomenology, and the statistical uncertainty of our plateau-average result at $t_{\mathrm{sep}} \approx 0.7 \ldots 0.8$ fm is comparable to previous experiments. One notable exception is the G_E/G_M ratio for the neutron at small $Q^2 \lesssim 2\,\mathrm{GeV}^2$. This disagreement is likely attributable to excited state contamination. Indeed, since our momentum-smeared nucleon operators are optimized for overlap with the ground state in the Breit frame, they become poorly optimized when the source momentum is near zero, i.e. $Q^2 \lesssim \frac{1}{4}Q^2_{\mathrm{max}}$.

5. Summary/outlook

In this report, we present our preliminary results from high-statistics calculations of the proton and neutron electromagnetic form factors at high momentum up to $Q^2 \approx 8\mathrm{GeV}^2$. We evaluate both connected and disconnected quark contributions at two different lattice spacings and two pion masses, one of which is very close to the physical point. Our preliminary analysis indicates that

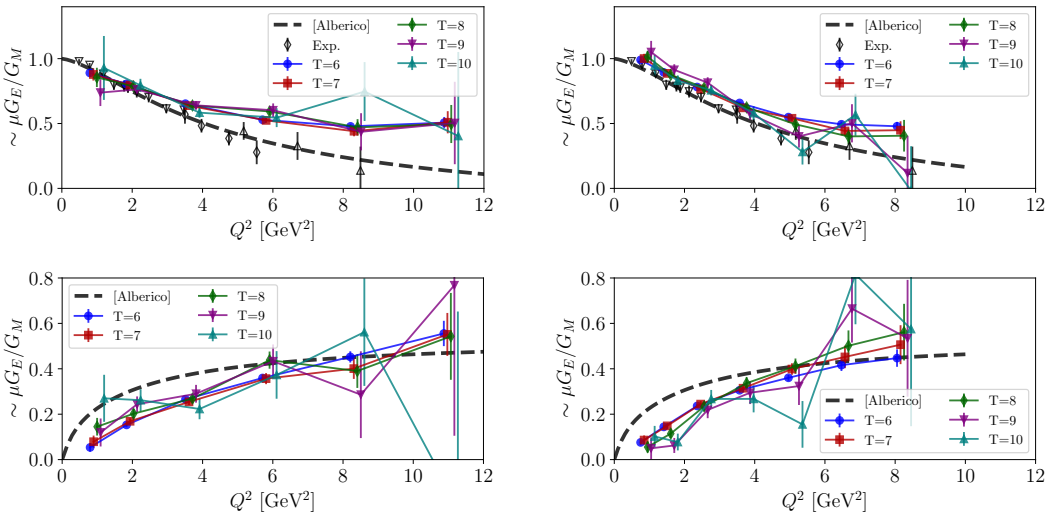

Figure 5: Ratio of the form factors G_E/G_M of the proton (top) and neutron (bottom) on the D5 ($m_\pi \approx 280$ MeV, left) and D6 ($m_\pi \approx 170$ MeV, right) ensembles. Both connected and disconnected contributions are included. The black data points are experimental values and the dashed lines are phenomenological fits [17]

stochastic uncertainty due to disconnected contributions can be constrained to $\lesssim 20\%$ for the proton and neutron form factors but it will be more challenging in the cases of individual flavors. Our current results pave the way for a complete calculation of high-momentum form factors that will be compared to the new data obtained at JLab.

Acknowledgments

S.S. is supported by the National Science Foundation under NSF award PHY 2412963. Any opinions, findings, and conclusions or recommendations expressed in this material are those of the author(s) and do not necessarily reflect the views of the National Science Foundation. M.E., J.N. and A.P. are supported by the U.S. DOE, Office of Science, Office of Nuclear Physics through grants numbered DE-FG02-96ER40965, DE-SC-0011090 and DE-SC-0023116, respectively. S.K. is supported by the MKW NRW under funding code NW21-024-A. The research reported in this work made use of computing and long-term storage facilities of the USQCD Collaboration, which are funded by the Office of Science of the U.S. Department of Energy. The authors gratefully acknowledge the Gauss Centre for Supercomputing e.V. (www.gauss-centre.eu) for funding this project by providing computing time through the John von Neumann Institute for Computing (NIC) on the GCS Supercomputer JUWELS at Jülich Supercomputing Centre (JSC). We are grateful to our JLab/W&M, LANL, and MIT colleagues for supplying dynamical Wilson-clover gauge configurations for this study. This research also used resources of the National Energy Research Scientific Computing Center, a DOE Office of Science User Facility supported by the Office of Science of the U.S. Department of Energy under Contract No. DE-AC02-05CH11231 using NERSC award NP-ERCAP0024043. The computations were performed using the Qlua software suite [20].

References

[1] V. Punjabi, C.F. Perdrisat, M.K. Jones, E.J. Brash and C.E. Carlson, *The Structure of the Nucleon: Elastic Electromagnetic Form Factors*, *Eur. Phys. J.* **A51** (2015) 79 [1503.01452].

[2] Z.-F. Cui, C. Chen, D. Binosi, F. de Soto, C.D. Roberts, J. Rodríguez-Quintero et al., *Nucleon elastic form factors at accessible large spacelike momenta*, *Phys. Rev. D* **102** (2020) 014043 [2003.11655].

[3] J. Arrington, E. Christy, S. Gilad, B. Moffit, V. Sulkosky, B. Wojtsekhowski et al., "Precision Measurement of the Proton Elastic Cross Section at High Q^2." https://www.jlab.org/exp_prog/proposals/07/PR12-07-108.pdf, 2007.

[4] E. Brash, E. Cisbani, M. Jones, M. Khandaker, N. Liyanage, L. Pentchev et al., "Large Acceptance Proton Form Factor Ratio Measurements at 13 and 15 $(\mathrm{GeV}/c)^2$ Using Recoil Polarization Method." https://www.jlab.org/exp_prog/proposals/07/PR12-07-109.pdf, 2008.

[5] G. Cates, S. Riordan, B. Wojtsekhowski et al., "Measurement of the Neutron Electromagnetic Form Factor Ratio G_{En}/G_{Mn} at High Q^2." https://www.jlab.org/exp_prog/proposals/09/PR12-09-016.pdf, 2009.

[6] J. Annand, R. Gilman, B. Quinn, B. Wojtsekhowski et al., "Precision measurement of the Neutron Magnetic Form Factor up to $Q^2 = 18.0(\mathrm{GeV}/c)^2$ by the Ratio Method." https://www.jlab.org/exp_prog/proposals/09/PR12-09-019.pdf, 2009.

[7] W. Brooks, J. Lachniet, M. Vineyard et al., "Measurement of the Neutron Magnetic Form Factor at High Q^2 Using the Ratio Method on Deuterium." https://www.jlab.org/exp_prog/proposals/07/PR12-07-104.pdf, 2007.

[8] M.E. Christy et al., *Form Factors and Two-Photon Exchange in High-Energy Elastic Electron-Proton Scattering*, *Phys. Rev. Lett.* **128** (2022) 102002 [2103.01842].

[9] UKQCD, QCDSF, CSSM collaboration, *Electromagnetic form factors at large momenta from lattice QCD*, *Phys. Rev.* **D96** (2017) 114509 [1702.01513].

[10] G.P. Lepage, "The analysis of algorithms for lattice field theory." Invited lectures given at TASI'89 Summer School, Boulder, CO, Jun 4-30, 1989, 1989.

[11] S. Syritsyn, A.S. Gambhir, B. Musch and K. Orginos, *Constructing Nucleon Operators on a Lattice for Form Factors with High Momentum Transfer*, *PoS* **LATTICE2016** (2017) 176.

[12] C. Kallidonis, S. Syritsyn, M. Engelhardt, J. Green, S. Meinel, J. Negele et al., *Nucleon electromagnetic form factors at high Q^2 from Wilson-clover fermions*, *PoS* **LATTICE2018** (2018) 125 [1810.04294].

[13] S. Syritsyn, M. Engelhardt, J. Green, S. Krieg, J. Negele and A. Pochinsky, *Nucleon Electromagnetic Form Factors at Large Momentum Transfer from Lattice QCD*, *Few Body Syst.* **64** (2023) 72.

[14] G.S. Bali, B. Lang, B.U. Musch and A. Schäfer, *Novel quark smearing for hadrons with high momenta in lattice QCD*, *Phys. Rev.* **D93** (2016) 094515 [1602.05525].

[15] J. Green, S. Meinel, M. Engelhardt, S. Krieg, J. Laeuchli, J. Negele et al., *High-precision calculation of the strange nucleon electromagnetic form factors*, *Phys. Rev.* **D92** (2015) 031501 [1505.01803].

[16] S. Syritsyn, J. Bratt, M. Lin, H. Meyer, J. Negele et al., *Nucleon Electromagnetic Form Factors from Lattice QCD using 2+1 Flavor Domain Wall Fermions on Fine Lattices and Chiral Perturbation Theory*, *Phys.Rev.* **D81** (2010) 034507 [0907.4194].

[17] W.M. Alberico, S.M. Bilenky, C. Giunti and K.M. Graczyk, *Electromagnetic form factors of the nucleon: New Fit and analysis of uncertainties*, *Phys. Rev.* **C79** (2009) 065204 [0812.3539].

[18] A.S. Gambhir, A. Stathopoulos, K. Orginos, B. Yoon, R. Gupta and S. Syritsyn, *Algorithms for Disconnected Diagrams in Lattice QCD*, *PoS* **LATTICE2016** (2016) 265 [1611.01193].

[19] A.S. Gambhir, A. Stathopoulos and K. Orginos, *Deflation as a Method of Variance Reduction for Estimating the Trace of a Matrix Inverse*, *SIAM J. Sci. Comput.* **39** (2017) A532 [1603.05988].

[20] A. Pochinsky, "Qlua lattice software suite." https://usqcd.lns.mit.edu/qlua, 2008–present.